J. Fluid Mech. (1988), *vol.* 190, *pp.* 427–450
Printed in Great Britain

Do large structures control their own growth in a mixing layer? An assessment

By UPENDER K. KAUL
Sterling Federal Systems (Palo Alto), NASA Ames Research Center, Moffett Field, CA 94035, USA

(Received 29 July 1986 and in revised form 24 May 1987)

This study makes a specific comparison between two different two-dimensional free shear layers: the T-layer which develops in time from an initial tangential velocity discontinuity separating the two half-spaces; and the S-layer which develops downstream of the origin where two uniform streams of unequal velocity are brought into tangential contact. The method of comparison is to assume that the vorticity of the S-layer is given parabolically by a Galilean mapping of that of the T-layer; to satisfy the appropriate boundary conditions in the S-layer and to compute the velocity induced at any point in the S-layer by its vorticity field; and to compare this velocity to that which can be derived from the velocity of the T-layer at corresponding points by a Galilean transformation of the velocity itself. The purpose of this calculation is to assess approximately how far the flow in the S-layer is from parabolic and, in particular, to what extent the perturbations induced upstream by large concentrations of vorticity found downstream are instrumental in hastening or retarding the subharmonic instability that leads to the formation of these large structures. The calculations suggest that this elliptic influence, or the feedback, in a mixing layer is relatively small, at least for small velocity ratios.

1. Introduction

A shear layer is formed whenever two streams at different velocities come in contact with each other. In nature it is found, for example, in the discharge of a river in a lake or an estuary, or in those regions in the atmosphere where clear-air turbulence is encountered. In the laboratory, the spatial development of a shear layer formed downstream of the trailing edge of a thin splitter plate, a plane jet or a backward-facing step has been the subject of many experimental investigations. It has been studied in detail in the laboratory by Liepman & Laufer (1947), Bradshaw (1966), Freymuth (1966), Browand (1966), Brown & Roshko (1974), Winant & Browand (1974), Batt (1975), Pui & Gartshore (1978), Ho & Huang (1982), among others. This real turbulent shear layer, hereafter referred to as the S-layer (see figure 1*a*), is a turbulent flow endowed with a well-documented large-scale coherent structure which persists over a wide range of Reynolds numbers. A notable feature of this coherent motion is its close similarity to the two-dimensional unsteady flow that arises from the initial superposition of two uniform streams at different speeds and a few initially weak two-dimensional perturbations. In the latter case, to define the initial flow field, infinitesimal perturbation theory is used. It yields eigenfunctions for the velocity components which are satisfactory solutions of the equations of motion as long as their amplitude is sufficiently small. The eigenfunctions selected are those that according to linear stability theory have the largest growth rate,

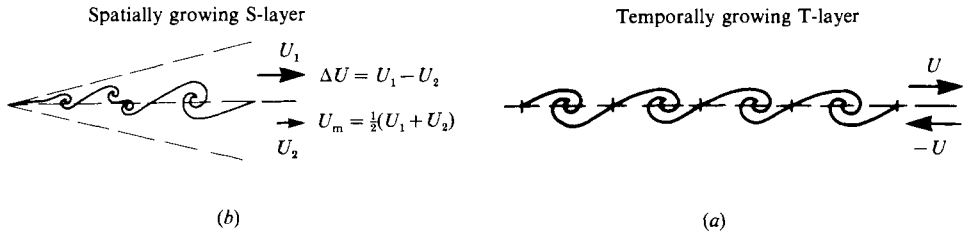

FIGURE 1. (*a*) Schematic of a spatially growing mixing layer, the S-layer, at some given time t'. (*b*) Schematic of a temporally growing mixing layer, the T-layer, at some given time t.

together with subharmonics of these waves which will grow slowly at first but which will amplify rapidly during the nonlinear stage of the calculation. The growing (fundamental) perturbations develop into a row of connected vorticity spirals whose spacing is the fundamental wavelength. These spirals, being unstable to subharmonic perturbations, subsequently pair and as a result both the circulation around a spiral and the spacing between the adjacent spirals increase. The results of numerical computations under such controlled initial conditions and periodic boundary conditions by Patnaik, Corcos & Sherman (1976), Peltier, Halle & Clarke (1978) and Riley & Metcalfe (1980) illustrate this phenomenon.

To what extent the coherent motion in the S-layer can be approximated by this deterministically calculable two-dimensional unsteady flow, hereafter referred to as the T-layer (see figure 1*b*), is discussed in Corcos (1979) and Corcos & Sherman (1984). Essentially, the deviations from the two-dimensionality of a real shear layer are viewed as perturbations (though possibly large) of this basic two-dimensional time-dependent flow in the sense that their interaction with that flow is apparently unable to destroy or even to control it. Accordingly, such a two-dimensional flow can be treated as a base flow for the turbulent mixing layer. This base flow is, therefore, proposed as a substitute (Corcos 1979) for the usual mean flow of turbulence. This results in a very marked simplification in that this base flow has an independent existence, whereas the mean flow does not.

Comparison of the calculations of the T-layer with the experimental studies by Brown & Roshko (1974) and Winant & Browand (1974) of the plane turbulent mixing layer, and with the subsequent analysis by Jiménez (1980) of former's results, shows that the dynamics of the coherent motion in the T- and S-layers is essentially the same. In the S-layer, figure 1(*a*), the vortex sheet formed downstream of the trailing edge of the plate is seen to roll-up into discrete vortex cores or structures, and then these structures amalgamate essentially in pairs further downstream. The spacing between the newly paired vortex structures increases, and so does their diameter and hence the circulation around them. The only laboratory evidence of the initial stages of the growth of the T-layer to the author's knowledge lies in the tilting-tube experiment of Thorpe (1971), where the uniformity of the initial state in x and the antisymmetry of the flow with respect to the x-axis guarantees no propagation of the waves in x but only their growth in time up to a roll-up (see figure 1*b*).

In spite of the striking similarity between the T-layer and the S-layer flows, there are some differences between the two which have not been sufficiently explored so far. In the T-layer, the problem is parabolic in time and therefore the initial perturbation can be specified. In the S-layer, the problem is elliptic in space, and therefore it is not clear that the perturbations can be specified at the origin of the layer. Using the vortex method of Chorin (1973) for an S-layer, Ashurst (1977) does

in effect prescribe vorticity at the origin of this flow, but the size of the error that results is not clear. In fact, for the S-layer, none of the necessary boundary conditions are known *a priori* for a domain, $x' > 0, |y'| < \infty$, though if the domain is extended to negative values of x', one may assume reasonably that as $x' \to -\infty, \bar{\boldsymbol{u}} \to \bar{\boldsymbol{e}} \times \boldsymbol{U}_1$ for $y' > 0$, and $\bar{\boldsymbol{u}} \to \bar{\boldsymbol{e}} \times \boldsymbol{U}_2$ for $y' < 0$.

Recently, Davis & Moore (1985) in their numerical study of mixing layers used a quadratic upwind differencing for convective terms and a Leith-type differencing for time rate-of-change terms to solve the governing equations. They perturbed the flow near the origin by prescribing the eigenfunctions for an upstream hyperbolic tangent profile from the linear stability theory (see Monkewitz & Huerre 1982). It was necessary to impose some sort of a perturbation near the origin to trigger a roll-up as well as pairing processes at low Reynolds numbers. They found that whereas the dynamics of the mixing layer was insensitive to the magnitude of the Reynolds number, the shape of the vortices was dependent on it. The vortices were smeared owing to the physical diffusion as the Reynolds number was decreased. Also, the basic vortex dynamics was seen to be weakly dependent on the amplitudes of these perturbations, as also experimentally observed by Freymuth (1966) in his study of transition in a separated laminar boundary layer, and the frequency content detemined the dynamics of the shear layer, in agreement with the latter's experiment. To detect the presence of feedback, they perturbed the S-layer for some brief initial interval and then stopped the forcing to see if the vortices did roll-up. They thus found that the feedback was present only for cases where the Reynolds number was high and the upstream velocity profile was very unstable. This indicates that the physical diffusion retards this roll-up process in the absence of any external perturbations. The feedback considered by Davis & Moore (1985) was with respect to the roll-up process and not the pairing process, which is the result of a dynamically very different mechanism of the subharmonic instability. However, this raises a question as to whether the upwind-differencing techniques that must introduce some numerical diffusion may mask or misrepresent the feedback.

In another recent numerical study of free shear layers by Fujiwara, Taki & Arashi (1986), the authors employed an upwind-difference scheme such that the truncation-error term was of third order with the fourth derivative term as its coefficient. Using such a scheme and by carefully comparing the viscous-shear-stress terms with the third-order error term, they obtained physically meaningful solutions. They had tried other upwind-difference schemes that were not able to trigger the roll-up process, but with this particular scheme, they managed to trigger the roll-up and the pairing processes without any external forcing. This leads to an interesting inference that the spatial–temporal truncation-error terms of some finite-difference schemes may have the appropriate spectral content in them to provide the required forcing. If that is the case, a Fourier analysis of these error terms and their comparison with the eigensolutions from the linear theory should resolve this question. Even if it were so, the particular finite-difference scheme would provide the necessary perturbations only for a narrow range of flow parameters. Conversely, even if one were to impose the perturbations from the linear stability theory, they could be swamped by the truncation-error terms of a particular finite-difference scheme.

This should explain why the calculation of the T-layers has been far more popular, since the streamwise direction is not finite differenced but Fourier transformed. Also, computer storage required for the S-layer calculations is an order of magnitude larger.

One of the physical questions associated with this difference between the T- and

S-layers is the following: can the distant vortices, which have already paired once or several times downstream in the S-layer, induce perturbations upstream that seed the subharmonic instability? In this case, the S-layer would not need imposed upstream perturbations in order to develop downstream, but would create its own perturbations and keep developing downstream.

In order to quantify such a question, the present work offers a model of the S-layer which introduces the elliptic nature of the real flow indirectly to some level of approximation into a solution of the T-layer.

2. Temporal problem

The problem in the temporal domain corresponds to the solution of two-dimensional unsteady Navier–Stokes equations and the continuity equation in an unbounded domain on a Cartesian (x, y)-grid. Spatial periodicity is enforced in the x-direction to allow the temporal evolution of wave-like structures. The base flow is assumed to be the diffused erstwhile tangential velocity discontinuity so that it is described by an error-function profile. At time $t = 0$ an appropriate perturbation field is imposed on this base flow and the flow is thus allowed to evolve. The initial perturbation field is given by

$$\Psi = \sum_{k=1}^{n} \mathrm{Re}\,[\Phi_k(y) \exp\{\mathrm{i}\alpha_k(x - c_k t)\}], \tag{1}$$

where $t = 0$; $\Phi(y)$ is the complex amplitude of the perturbation stream function calculated from the linear stability theory; $c = c_\mathrm{r} + \mathrm{i}c_\mathrm{i}$ is the complex phase speed with $c_\mathrm{r} = 0$ owing to the antisymmetry of the base profile, and $\alpha = \alpha_\mathrm{r}$ is the wavenumber of a given unstable mode k.

Computations in the T-layer are carried out with an initial perturbation composed of three normal modes. These normal-mode solutions are obtained by solving the linear stability problem. Since we are interested in the development of a mixing layer through the process of pairing and not a collective coalescence, only three wavenumbers, the fundamental and its first and third subharmonics were chosen; as a result two *successive* pairings are simulated. The fundamental wavenumber is selected to be the one that would be most amplified according to the linear theory. Initial amplitudes of the three wavenumbers are chosen sufficiently small for the linear stability theory to hold.

Contour plots of the passive scalars are shown in figure 2(*a–c*). The ordinates are shown in units of the fundamental wavelength λ_0. From these plots, it is seen that as the vortices pair, the diameter of the vortex spiral d doubles. Since the velocity U remains unchanged, the stretching rate γ, defined as $\partial_s u_s$, where s is the coordinate along the stagnation streamline joining two vortex spirals, being of the order of U/d, is halved for each pairing. The thickness of the individual vortex sheet δ is of the order $(\nu/\gamma)^{\frac{1}{2}}$ (see Corcos 1979; Corcos & Sherman 1976), and hence δ/d decreases by a factor of $\sqrt{2}$. Since time for each successive pairing doubles, we have therefore in time t, $\delta/d \propto 1/t^{\frac{1}{2}}$. This is the reason that the vorticity decreases at a slower rate than the rate at which the lengthscales increase for each pairing. Figure 3 shows the growth of the vorticity thickness $\delta_\omega = \Delta U/(\partial_y \bar{u})_0$ in the T-layer with time t; U is the reference velocity in the T-layer.

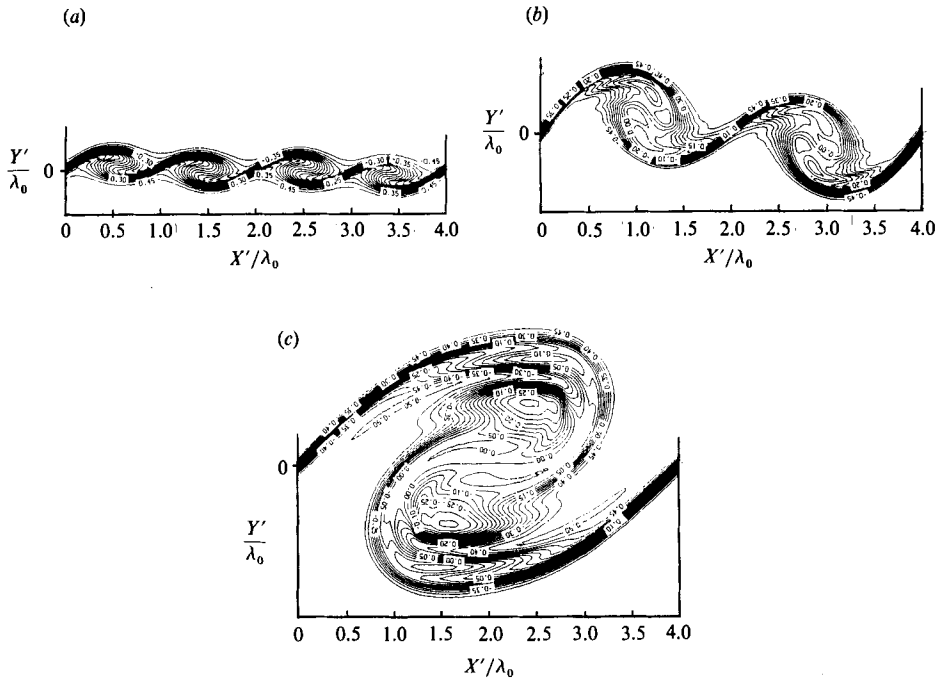

FIGURE 2. Passive-scalar contours in the T-layer, $Re_{\delta u_0} = 50$. Three-wave interaction: $\alpha_0 = 0.43$, $\alpha_1 = 0.215$, $\alpha_3 = 0.1075$; $A_0/A_1 = 2$; $A_0/A_3 = 4$. (*a*) Rolled-up structures; (*b*) once-paired structures; (*c*) twice-paired structure.

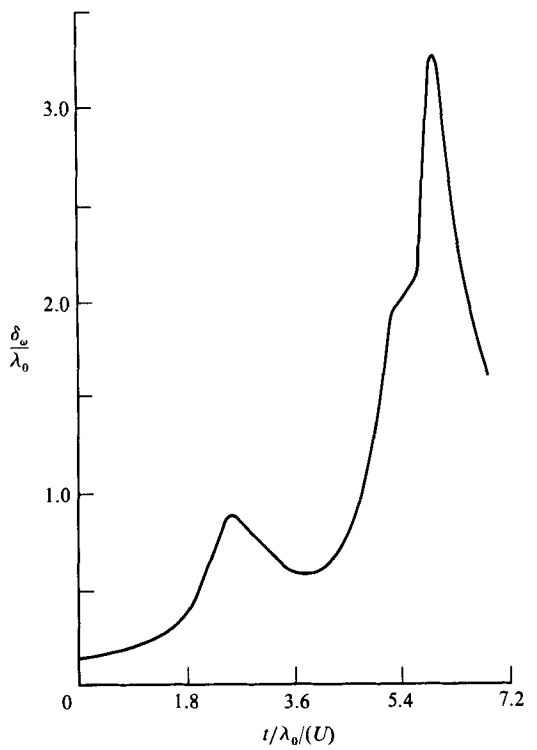

FIGURE 3. Growth of vorticity thickness with time in the T-layer. Three-wave interaction.

3. Spatial problem

In view of the dynamic similarity of the evolution of the structures in the T-layer with time t, and in the S-layer with downstream distance x', and the fact that these vortex structures move at a constant speed (sometimes called the celerity, see Coles 1985) equal to the mean speed U_m of the two streams in the S-layer, transformations are proposed in this study that will yield approximately the vorticity of the S-layer in terms of that of the T-layer. These transformations have roots in the following physical argument.

Let x', y', t' be the streamwise, cross-stream and time coordinates, respectively, in the S-layer corresponding to the coordinates x, y, t in the T-layer. If we conceive of an observer (x, y) in the T-layer moving along x at the mean speed U_m of the corresponding S-layer, while the initial perturbations grow through the linear range to a nonlinear range to an eventual roll-up and the subsequent pairings, he will have recorded all the vorticity fluctuations that passed him during this time interval, say, $t \in [0, T]$. This corresponds in the S-layer to a record of vorticity fluctuations over the space interval $x' \in [0, U_m T]$ at $y' = y, t' = t'_0$, a constant. Consider now a column of observers (x, y), $y \in (-\infty, \infty)$ at time $t = 0$, in the T-layer, who repeat this experiment simultaneously. We will have thus constructed a two-dimensional vorticity field $\omega'(x', y', t'_0)$ for the S-layer from $x' = 0$ to $x' = U_m T$, $y' \in (-\infty, \infty)$. This vorticity field is just one sample out of an infinite number of such possible samples corresponding to an infinite number of such columns of observers in any interval, say, $x \in [\mp 2^n \lambda_0, 0]$ in the T-layer at $t = 0$; n is the lowest subharmonic of the fundamental wavenumber of wavelength λ_0 present in the initial perturbation spectrum at $t = 0$ in the T-layer. Each sample S corresponds to a characteristic $x_s = \pm U_m t \mp x_{0s}$ in the (x, t)-plane of the T-layer and is a solution at that particular time $t' = t \mp x/U_m$ in the S-layer, see figure 4(a, b); x_{0s} is the intercept on the x-axis of the particular sample S as shown. These transformations include the one that was discussed in Corcos (1980) and Kaul (1982). The alternative mapping was used in a recent calculation (see Kaul 1986), and the corresponding results are discussed here.

Then, any property in the T-layer given by a function $f(x, y, t)$ will map into a corresponding function $f'(x', y', t')$ in the S-layer with the following linear transformations:

$$x' = U_m t, \quad t' = t \mp x/U_m, \quad y' = y. \tag{2}$$

Under this transformation, any finite region in the T-layer transforms into a corresponding finite region in the S-layer since the Jacobian of this linear transformation is given by

$$|J_z| = \left\| \frac{\partial(x', t', y')}{\partial(x, t, y)} \right\| = 1 \mp 0.$$

The vorticity equation in the T-layer transforms under this mapping to that for the S-layer as follows. The vorticity equation in the T-layer is governed by the equation

$$\partial_t \omega + u \partial_x \omega + v \partial_y \omega = \nu(\partial_{xx} \omega + \partial_{yy} \omega).$$

Using (2) and expressing it in terms of x', y', t', we first get the following equation for the S-layer:

$$\left(1 \mp \frac{u}{U_m}\right) \partial_{t'} \omega' + U_m \partial_{x'} \omega' + v' \partial_{y'} \omega' = \nu \left(\frac{1}{U_m^2} \partial_{t't'} \omega' + \partial_{y'y'} \omega' \right). \tag{3}$$

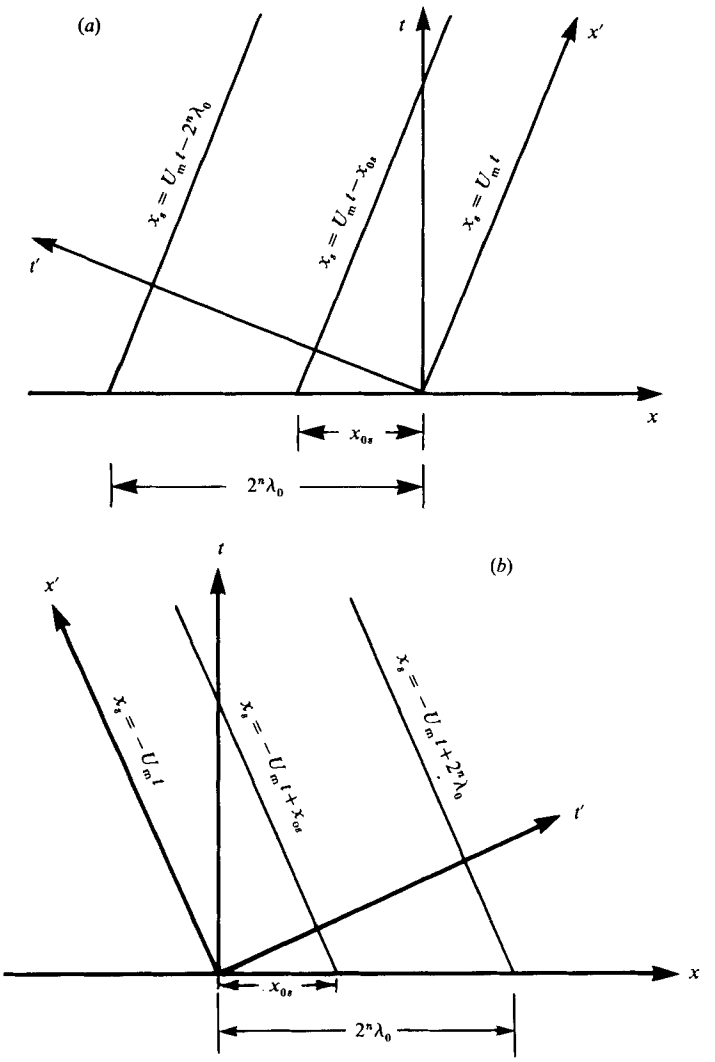

FIGURE 4. Coordinate axes system for the T- and the S-layers and the representation of $t' =$ constant as an (x,t) characteristic in the T-layer. (*a*) Transformation $t' = t - x/U_m$; (*b*) transformation $t' = t + x/U_m$.

Then if the Galilean transformation extends to u and v, we have

$$u' = u + U_m, \quad v' = v,$$

and we get

$$\left(1 \mp \frac{u' - U_m}{U_m}\right)\partial_{t'}\omega' + U_m\,\partial_{x'}\omega' + v'\,\partial_{y'}\omega' = \nu\left(\frac{1}{U_m^2}\partial_{t't'}\omega' + \partial_{y'y'}\omega'\right). \tag{4}$$

Now
$$u' = O\left[U_m\left(1 + \frac{\Delta U}{U_m}\right)\right] \to U_m \quad \text{as } \Delta U/U_m \to 0$$

and
$$\partial_{x'x'} = O\left\{\frac{1}{U_m + \Delta U}\partial_{t'}\right\}^2 \to \frac{1}{U_m^2}\partial_{t't'} \quad \text{as } \Delta U/U_m \to 0;$$

hence as $\Delta U/U_m \to 0$, the exact equation for the vorticity in the S-layer,

$$\partial_{t'}\omega' + u'\,\partial_{x'}\omega' + v'\,\partial_{y'}\omega' = \nu(\partial_{x'x'}\omega' + \partial_{y'y'}\omega'), \tag{5}$$

tends to (4).

These transformations map the vorticity of the T-layer to that of the S-layer accurately for small values of velocity ratios, $\Delta U/U_m$, where $\Delta U = U_2 - U_1$ and $U_m = \frac{1}{2}(U_1 + U_2)$, U_1 and U_2 being the velocities of the low- and high-speed streams respectively.

It is interesting to note that the transformations proposed here recover the relations derived by Gaster (1962, 1965) for the eigenvalues of the two domains for small rates of amplification. For example, on substituting the first of the transformations given by (2) into the expression $\exp\{i\alpha_r(x - ic_i t)\}$ or $\exp\{i(\alpha_r x - i\beta_i t)\}$, where $\beta_i > 0$ is the temporal amplification rate, corresponding to a single perturbation component in the T-layer (equation (1)), we get

$$\exp\left\{i\left[\left(\alpha_r - i\frac{\beta_i}{U_m}\right)x' - (\alpha_r U_m)\,t'\right]\right\}$$

in the S-layer, which can be rewritten as

$$\exp\{i[(a_r + ia_i)\,x' - b_r t']\},$$

where a_r is the wavenumber, $a_i < 0$ is the spatial amplification rate and b_r is the frequency. Comparing the preceding two expressons, we get $a_r = \alpha_r$, $a_i = -\beta_i/U_m$ and $b_r = \alpha_r U_m$. This implies that the wavenumbers in the two domains are equal and the group velocity $\partial b_r/\partial a_r$ is given by the ratio of the amplification factors in the two domains, $-\beta_i/a_i$.

According to our transformations, the mean speed or the celerity, U_m, is equal to the group velocity $\partial b_r/\partial a_r$. However, there is an error in these transformations which vanishes uniformly as $\Delta U/U_m \to 0$. In the T-layer, all the wavenumbers amplify without any dispersion. Therefore, this error is also a measure, in some sense, of the amount of dispersion between different wavenumbers as the perturbations travel downstream in the S-layer. In the case of naturally occurring mixing layers, however, these structures undergo a jitter with their most probable location given by a Gaussian distribution (see Brown & Roshko 1974). But, since the flow here is perturbed at the most amplified frequency together with its first and third subharmonics, we should expect an insignificant amount of dispersion beyond the stage of roll-up when the fundamental has saturated and the subharmonic begins to amplify rapidly. It is this region of the flow that is of most interest to us. That the fundamental and the subharmonic frequencies are phase locked when the subharmonic begins to amplify rapidly has been observed experimentally by Ho & Huang (1982) and is also suggested by the computational results of the author (Kaul 1986*b*). Now, since the space–time correlations would indicate that the celerity or the mean speed of the structures is not constant across the mixing layer and that it is biased in the direction of the mean velocity profile, it would appear that the transformations proposed here would be in error. But, it has been shown by Favre, Gaviglio & Dumas (1967) that this bias is only extraneous since it can be removed by filtering out the high-frequency component of the signals.

An order of magnitude analysis for the accuracy of the transformation (2) is carried out as follows.

In the S-layer, the vortices are carried downstream at a mean speed $U_m = \frac{1}{2}(U_1 + U_2)$, and also induce a velocity on themselves and on each other of the order

of $\Delta U = U_2 - U_1$. If $\Delta U/U_m \ll 1$, the dependence on time of the S-layer vorticity is given to first order by $\partial_{t'} = U_m \partial_{x'}$. Experimentally, even if $\Delta U/U_m$ is not small, the streamwise growth rate of the layer, i.e. the mean angle which it makes, is relatively small and therefore the development in space is relatively slow so that apparently, while the characteristic timescale in the S-layer is $d/\Delta U$, the timescale for a typical pairing is several units of $d/\Delta U$. From the two-dimensional calculations, with $\lambda \approx 3d$ and pairing time $\approx 2\lambda/\Delta U \approx 6d/\Delta U$, the error on the approximation above is roughly $\Delta U/6U_m$, rather than $\Delta U/U_m$.

Owing to the non-uniform distribution of vorticity in the streamwise direction in the S-layer, there is a finite net induced effect present at any point upstream in the S-layer. This is also a measure of the ellipticity of the S-layer problem. The difference between this induced velocity and the velocity transformed directly from the T-layer at a given point upstream will give a measure of the feedback signal. However, in constructing the S-layer vorticity field, the induced normal velocity upstream of the geometric origin of the flow has to be cancelled out to simulate the presence of the splitter plate. A method to do this is presented below. Other boundary conditions in the S-layer are satisfied by placing vortex sheets of appropriate strength in the flow field. Having thus completed the specification of the S-layer vorticity field, the feedback signal is measured at various upstream locations.

Frequency and power-spectra analyses are carried out to measure the amplitude and phase of the various components of the feedback signal and its effect on the fundamental and the first subharmonic (also the first and third subharmonics) of the transformed velocity itself.

3.1. *Boundary conditions in the S-layer*

The vorticity distribution $\omega'(x', y', t')$ obtained as described above is not by itself an acceptable approximate representation for the vorticity in the S-layer. The latter is necessarily characterized, in addition to a diffuse vorticity distribution which extends around the x'-axis to $x' \to \infty$, by a vorticity distribution for $x' < 0$ such that as $x' \to -\infty$ that distribution tends to a singular vortex sheet of strength ΔU per unit length, such that the induced velocity due to the total vorticity distribution has zero normal component for all points $x' \leqslant 0$ to simulate the flow over a splitter plate.

We shall be interested mostly in the contribution of the induced velocity to the first subharmonic frequency of the original fundamental frequency. As the vortices pair, the dominant contribution they make to the induced field is distributed over a few harmonics of their fundamental frequency, which is halved for each pairing. Thus while a large vortex far downstream of the trailing edge induces a field of velocity that is as intense as a smaller one further upstream, the same is not true of their relative contribution at a fixed frequency. Hence far enough downstream we replace the vorticity distribution by a simple steady vortex sheet of strength ΔU per unit length.

Since the boundary layer on the splitter plate is thin in the experiments, we tend to think of the vorticity distribution for $x' \leqslant 0$ as a singular vortex sheet whose density $\Gamma(x')$ tends to ΔU as $x' \to -\infty$.

The total vorticity distribution is sketched in figure 5. By adding a uniform velocity field $u = U_m$ everywhere, the boundary condition at $y' = \pm\infty$ will thus be satisfied. A distribution $\Gamma(x')$ is determined on the splitter plate $x' \leqslant 0, y' = 0$ in order to satisfy the condition $v' = 0$ there. To do this we proceed as follows.

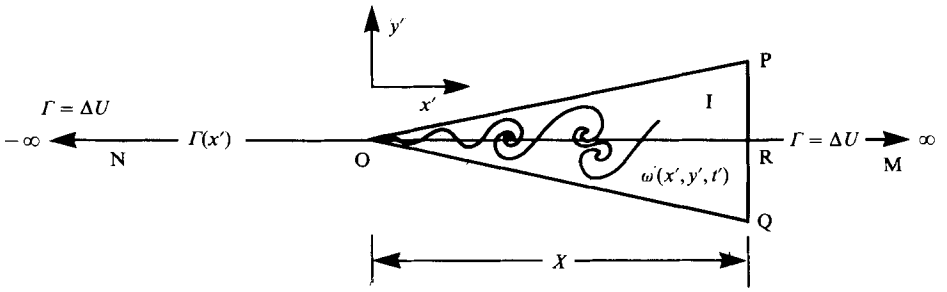

FIGURE 5. Model of the S-layer; vorticity at a given time t'.

3.1.1. *Boundary condition on the plate*

For all practical purposes, we can consider a finite distance ON, figure 5, beyond which the vortex density $\Gamma(x')$ assumes a constant value ΔU. This is the distance over which the induced normal velocity due to the vorticity distribution for $x' > 0$ will have decayed to a negligible value. Thus we determine $\Gamma(x')$ for $x_N < x' \leqslant 0$, with $\Gamma(x') = \Delta U$ for $x < x_N$. The segment ON can be thought of as the splitter plate whose leading edge N is far enough away such that any perturbations there have a negligible effect on the flow near the trailing edge O. This is similar to the concept in the theory of thin airfoils where the leading-edge effects are ignored while replacing the airfoil by a vortex sheet of variable density whose induced velocity field cancels the normal velocity created by the camber of the airfoil and its angle of attack. The solution adopted here is similar in spirit to the one used there with the difference that the induced normal velocity here is due to the non-uniform distribution of vorticity for $x' > 0$ and that its functional form is not easily handled in the numerical technique.

Shift the origin $x' = 0$ by a distance $\frac{1}{2}a$ upstream to the midpoint of the plate, and replace the splitter plate by a vortex sheet extending over the interval $-\frac{1}{2}a \leqslant x' \leqslant \frac{1}{2}a$, of some unknown vortex density $\Gamma(x')$. Distance a is sufficiently large that the induced normal velocity v_I due to the region I (figure 5) is negligible at $x' = -\frac{1}{2}a$. This induced normal velocity v_I at any point x' on the vortex sheet $\Gamma(x')$ must be balanced by an equal and opposite induced normal velocity v_Γ at that x' due to the vorticity distribution over the entire vortex sheet. This condition along with the Kutta condition, i.e. the velocity at the trailing edge of the plate $x' = \frac{1}{2}a$ is finite, will be the basis for our determination of the vortex density $\Gamma(x')$. We are still left with an infinite velocity at the leading edge of the plate $x' = -\frac{1}{2}a$, but as in thin airfoil theory, the solution obtained thus will be accurate enough for our purposes here.

Once the vortex density $\Gamma(x')$ is determined, the total induced velocity at any point in the flow field will be the resultant of the induced velocities due to (*a*) the region I, (*b*) the non-uniform vortex sheet $\Gamma(x')$, (*c*) the uniform vortex sheet of strength ΔU, $-\infty < x' < \frac{1}{2}a$, and lastly, (*d*) the uniform vortex sheet of density ΔU, $(\frac{1}{2}a + X) \leqslant x' < \infty$ (see figure 5).

Thus we shall proceed as follows. The unknown vortex density $\Gamma(x')$, $-\frac{1}{2}a \leqslant x' \leqslant \frac{1}{2}a$, is subject to the two conditions

(i) $$v_\Gamma(x') + v_I(x') = 0; \quad -\tfrac{1}{2}a \leqslant x' \leqslant \tfrac{1}{2}a,$$

where $$v_\Gamma(x') = \frac{1}{2\pi}\int_{-\frac{1}{2}a}^{\frac{1}{2}a} \frac{\Gamma(\xi)}{x' - \xi}\,\mathrm{d}\xi$$

and (ii) the trailing edge velocity, $q_{x'=\frac{1}{2}a}$, is finite.

Then we can write

$$\frac{1}{2\pi}\int_{-\frac{1}{2}a}^{\frac{1}{2}a}\frac{\Gamma(\xi)}{x'-\xi}\mathrm{d}\xi = -v_{\mathrm{I}}(x'), \tag{6}$$

with $x' \in [-\frac{1}{2}a, \frac{1}{2}a]$ and

$$\Gamma(x') = 0 \quad \text{at } x' = \tfrac{1}{2}a. \tag{7}$$

Integral (6) subject to (7) yields an analytical solution if the function $v_{x'}$ can be expanded in a Fourier series. Condition (7) ensures that the trailing-edge velocity is finite.

Using the transformations

$$x' = -\tfrac{1}{2}a\cos\theta, \quad \xi = -\tfrac{1}{2}a\cos\phi,$$

(6) and (7) become

$$\frac{1}{2\pi}\int_0^{\pi}\frac{\Gamma(\phi)\sin\phi}{\cos\phi-\cos\theta}\mathrm{d}\phi = -v_{\mathrm{I}}(\theta), \tag{8}$$

with $\theta \in [0, \pi]$, and

$$\Gamma(\phi) = 0 \quad \text{for } \phi = \pi. \tag{9}$$

Assume a solution of the form

$$\Gamma(\phi) = 2\left[\Gamma_0\left(\frac{1+\cos\phi}{\sin\phi}\right) + \Gamma_1\sin\phi + \Gamma_2\sin 2\phi + \ldots + \Gamma_n\sin(n\phi)\right], \tag{10}$$

where constants $\Gamma_0, \Gamma_1, \Gamma_2, \ldots, \Gamma_n$ will be determined by the Fourier expansion of the known function, $v_{\mathrm{I}}(\theta)$.

It can be seen on inspection that (10) automatically satisfies (9). Substituting (10) into (8) and using the integral formulae

$$\int_0^{\pi}\frac{\cos(n\phi)\sin\theta}{\cos\phi-\cos\theta}\mathrm{d}\phi = \pi\sin(n\theta), \quad n = 0, 1, 2, 3, \ldots$$

and

$$\int_0^{\pi}\frac{\sin(n\phi)\sin\phi}{\cos\phi-\cos\theta}\mathrm{d}\phi = -\pi\cos(n\theta), \quad n = 1, 2, 3, \ldots,$$

which are the corresponding Cauchy principal values, we arrive at

$$-\Gamma_0 + \Gamma_1\cos\theta + \Gamma_2\cos 2\theta + \ldots + \Gamma_n\cos(n\theta) = v_{\mathrm{I}}(\theta). \tag{11}$$

Expanding $v_{\mathrm{I}}(\theta)$ in a cosine Fourier series, let

$$v_{\mathrm{I}}(\theta) = v_0 + v_1\cos\theta + v_2\cos 2\theta + \ldots + v_n\cos(n\theta). \tag{12}$$

Comparing (11) and (12), we obtain

$$\Gamma_0 = -v_0, \quad \Gamma_n = v_n, \quad n = 1, 2, 3, \ldots. \tag{13}$$

With (13), we have the required solution for $\Gamma(\phi)$ from (10). The induced velocity due to the non-uniform vortex sheet is thus given by

$$u_{\Gamma} = \frac{1}{2\pi}\int_0^{\pi}\frac{\Gamma(\phi)\,y'}{(x'+\frac{1}{2}a\cos\phi)^2 + y'^2}\{\tfrac{1}{2}a\sin\phi\}\,\mathrm{d}\phi \tag{14}$$

and

$$v_{\Gamma} = \frac{-1}{2\pi}\int_0^{\pi}\frac{\Gamma(\phi)(x'+\frac{1}{2}a\cos\phi)}{(x'+\frac{1}{2}a\cos\phi)^2 + y'^2}\{\tfrac{1}{2}a\sin\phi\}\,\mathrm{d}\phi, \tag{15}$$

where

$$x' \notin [-\tfrac{1}{2}a, \tfrac{1}{2}a] \quad \text{for } y' = 0.$$

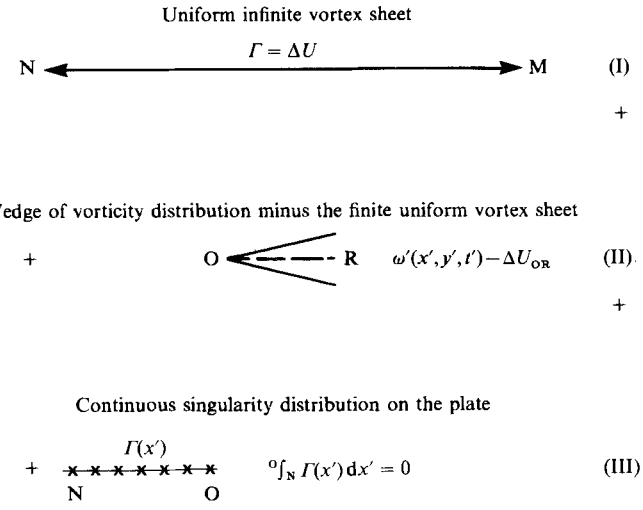

FIGURE 6. Various contributions to the total vorticity in the S-layer.

3.1.2. *Calculation of the induced velocity field*

Instead of calculating the induced velocities of the two uniform vortex sheets of strength ΔU, $-\infty < x' \leqslant \frac{1}{2}a$, and $(X+\frac{1}{2}a) \leqslant x' < \infty$, and the induced velocity due to the region I separately, the following procedure is adopted for simplicity.

Referring to figure 6, a uniform vortex sheet OR of strength ΔU, $\frac{1}{2}a < x' < (X+\frac{1}{2}a), y' = 0$, is subtracted from the vorticity distribution in region I. The induced normal velocity $v_I - v_{OR}$ is calculated on the splitter plate, $-\frac{1}{2}a \leqslant x' \leqslant \frac{1}{2}a$, and it is this velocity that is annulled on the plate rather than the velocity v_I. This in effect gives a small distance a in which the induced normal velocity $v_I - v_{OR}$ decays to negligible values, and hence a very efficient Fourier analysis of the function $v_I - v_{OR}$, and a simple superposition of a uniform infinite vortex sheet Γ_∞ of strength ΔU, $-\infty < x' < \infty$ instead. The induced velocity due to the vortex sheet OR is given by

$$u_{OR} = \frac{\Delta U}{2\pi} \int_{\frac{1}{2}a}^{X+\frac{1}{2}a} \frac{y'}{(x'-\xi)^2 + y'^2} d\xi$$

or

$$u_{OR} = \frac{\Delta U}{\pi} \arctan\left(\frac{x'-\xi}{y'}\right)\Bigg|_{\frac{1}{2}a}^{X+\frac{1}{2}a},$$

and

$$v_{OR} = \frac{-\Delta U}{2\pi} \int_{\frac{1}{2}a}^{X+\frac{1}{2}a} \frac{x'-\xi}{(x'-\xi)^2 + y'^2} d\xi$$

or

$$v_{OR} = \frac{-\Delta U}{4\pi} \ln\left[(x'-\xi)^2 + y'^2\right]\Big|_{\frac{1}{2}a}^{X+\frac{1}{2}a}.$$

3.2. *Sampling and power-spectrum analysis*

To measure the feedback effect, we calculate the velocity in the S-layer as discussed above and compare its harmonic content with that of the velocity mapped directly from the T-layer. Let $v'(t')$ be a velocity in t' at any (x', y'), with a periodicity over the interval $t' \in [0, T]$, where $T = 2^n T_0$, n being the number of pairings. This velocity

is constituted of n subharmonic frequencies, fundamental frequency and higher harmonics.

The velocity v' has an amplitude spectrum that is not monotonic in general. In doing a discrete Fourier analysis of v', therefore, it has to be ascertained that we do not get into the hazards of aliasing. Choosing the fundamental frequency f_0 as the Nyquist or the folding frequency we have, from the sampling theorem, the equispaced time interval for band-limited functions given by

$$\Delta t \leqslant \frac{1}{2(1/T_0)} = \tfrac{1}{2}T_0.$$

This means that we need to sample the values for $v'(t')$ at at least 2^{n+1} regular intervals.

In the T-layer different numbers of samples, equal to and greater than the number determined by the sampling theorem, were used to evaluate the effects of aliasing. Based on these results, a proper choice for the number of samples for the function $v'(t')$ in the S-layer was made.

3.3. *Error checks*

Apart from various diagnostic tests for accuracy, there are some important checks to be made on the computations in the S-layer. Once the transformations take us from the T-layer to the S-layer, we have a certain vorticity distribution in the region I (figure 5) which is subject to an integral condition:

$$\Gamma_{\mathrm{OPQO}} = \iint \omega' \,\mathrm{d}x' \,\mathrm{d}y' = X\,\Delta U.$$

Since the perturbation vortex sheet $\Gamma(x')$ cancels the induced velocity $v_{\mathrm{I}} - v_{\mathrm{OR}}$ on the plate, which arises from (a) the vorticity distribution in region I of total circulation $X\,\Delta U$ and (b) the vortex sheet OR of total circulation $X\,\Delta U$, the total circulation Γ_{T} around the perturbation vortex sheet should be equal to zero. A simple expression for the total circulation Γ_{T} can be derived as follows:

$$\Gamma_{\mathrm{T}} = \int_{-\frac{1}{2}a}^{\frac{1}{2}a} \Gamma(\xi)\, d\xi = \int_0^{\pi} \Gamma(\phi)\, \tfrac{1}{2}a \sin\phi \,\mathrm{d}\phi,$$

with

$$\xi = -\tfrac{1}{2}a\cos\phi,$$

or

$$\Gamma_{\mathrm{T}} = a\int_0^{\pi}\left[\Gamma_0\left(\frac{1+\cos\phi}{\sin\phi}\right) + \Gamma_1 \sin\phi + \Gamma_2 \sin 2\phi + \ldots + \Gamma_n \sin(n\phi)\right]\sin\phi\,\mathrm{d}\phi,$$

using (10), or,

$$\Gamma_{\mathrm{T}} = a\pi(\Gamma_0 + \tfrac{1}{2}\Gamma_1).$$

In view of (13), we have

$$\Gamma_{\mathrm{T}} = a\pi(\tfrac{1}{2}v_1 - v_0), \tag{16}$$

where v_0 and v_1 are given by (12) with its left-hand side replaced by $v_{\mathrm{I}}(\theta) - v_{\mathrm{OR}}(\theta)$.

If the solution (10) for the plate, the non-uniform vortex sheet $\Gamma(\phi)$, is unique, then the right-hand side of (16) should be zero. The vortex density $\Gamma(\phi)$ can be looked upon as a perturbation in the neighbourhood of the plate trailing edge $x' < \frac{1}{2}a$ over the uniform vortex sheet of strength ΔU that extends to $x' \to -\infty$.

The most important check in the present computations is to make sure that data are sampled at a sufficient number of points in carrying out the harmonic analysis of the function $v'(t')$, otherwise serious aliasing errors will occur. Since the amplitude

spectrum of $v'(t')$ is non-monotonic in general, any aliasing of higher frequencies will result in false amplitudes and phases of the frequencies of interest.

In the T-layer, an analysis was carried out with 128, 64, 32, 16 and 8 samples over the interval $x \in [0, 2^n \lambda_0]$. Sampling with the first three sets of points yielded amplitude spectra agreeing with one another up to four decimal places. Amplitude spectra with the fourth set, 16 samples, agreed with the previous ones to the third decimal place, whereas the last set gave a spectrum about 30% different from the previous ones in the range of frequencies of interest. With the value of $n = 2$, a proper choice for Δx would correspond to 8 samples according to the sampling theorem, which according to the analysis in the T-layer is insufficient. Therefore, our optimum choice for the number of samples is 16, which as mentioned before is satisfactory. This gives us an idea of the band-limitedness of the function $v(x)$ in the T-layer, that is, the function $v(x)$ is band-limited beyond the second harmonic of the fundamental, which corresponds in the S-layer to a frequency twice the fundamental frequency f_0.

3.4. *Results in the S-layer*

The computations are carried out corresponding to two values of velocity ratios and at a Reynolds number of 50 based on the initial shear-layer thickness. The values of $\Delta U/U_m$ are chosen as 2 and 0.666. The initial perturbations are chosen from the linear stability theory and the amplitude ratios between the fundamental and the subharmonics are progressively fixed at 2 so that each 'local fundamental' has a chance to amplify on its own before its subharmonic begins to overtake it. Four different time realizations of the flow pattern shown through the vorticity contours corresponding to $\Delta U/U_m = 0.666$ are shown in figure 7 (*a–d*). The same realizations are shown through passive-scalar contours in figure 8 (*a–d*). The initial stability, predominantly the fundamental, is seen to roll-up. Then the rolled-up structures coalesce further downstream. Still further downstream, the once-paired structures coalesce again. During this process of pairing, the spacing between and the scale of these structures is seen to approximately double as expected. The same interaction between the structures is seen in figure 9, which gives a time realization corresponding to $\Delta U/U_m = 2$. The pattern of passive-scalar contours shown in figure 10 (Plate 1) is strikingly similar to that of the structures observed by Brown & Roshko (1974), Winant & Browand (1974) and by others.

The induced velocity due to the distribution of vorticity in the S-layer on the splitter plate is plotted in figure 11 (*a*) for the case of $\Delta U/U_m = 2$ for a given t'. This vorticity perturbation is seen to decay to zero at upstream distances greater than a few fundamental wavelengths of the initial perturbation. The vortex-sheet (splitter-plate) density that will cancel this induced velocity is shown plotted along the length of the plate upstream in figure 11 (*b*).

While assessing the differences in the phase and amplitude between the calculations with and without feedback, it should be noted that if the initial perturbation at $x' = 0$ in the S-layer is the same as that in the T-layer at $t = 0$, then the velocity in the S-layer, $v'(t')$, and that transformed directly from the T-layer can be directly compared except that the phase change of the perturbation is linear in time t in the case of the latter. But, as is the case in the experiments, the splitter plate is held fixed in the present computations and the flow is imagined to be excited elsewhere, $x' = 0, y' \neq 0$. This gives a zero velocity v' at $x' = 0$ for all t'. Only some distance downstream of the trailing edge, $x' > 0, y' = 0$ will the flow perturbations have recovered from this effect and the comparison between v' and that mapped directly from the T-layer become meaningful.

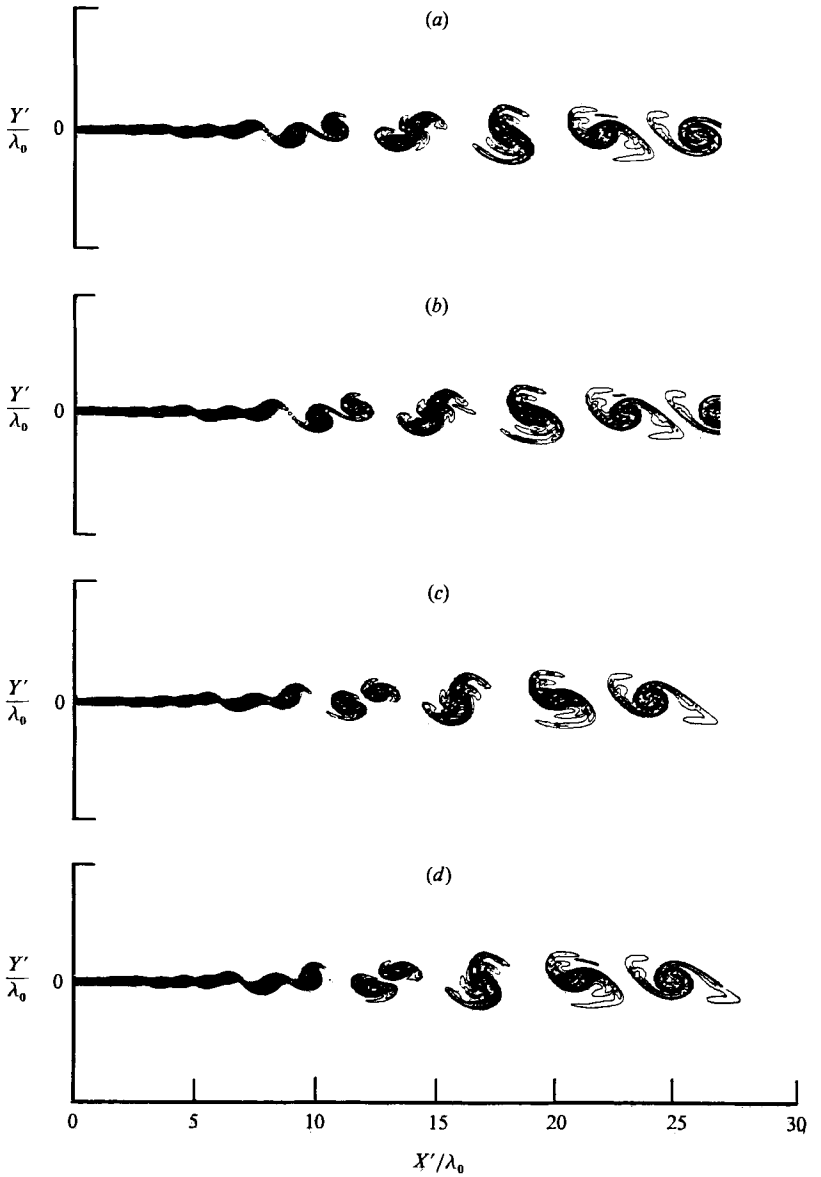

FIGURE 7. (*a–d*) Vorticity contours in the S-layer corresponding to four different time realizations; $\Delta U/U_m = 0.666$.

To quantify the feedback signal in the shear layer, the contribution corresponding to the subharmonic of the initial fundamental is measured upstream of the region where the first subharmonic reaches its peak or saturates. This includes the regions where the fundamental has rolled-up into a vortex structure, where the first subharmonic begins to dominate and where it eventually saturates. The relative change in amplitude of the first subharmonic is calculated along with the change in the phase difference between this subharmonic and its fundamental. The change in the phase difference is calculated relative to the phase shift that would inhibit the subharmonic instability. These results are plotted in figure 12 for various downstream

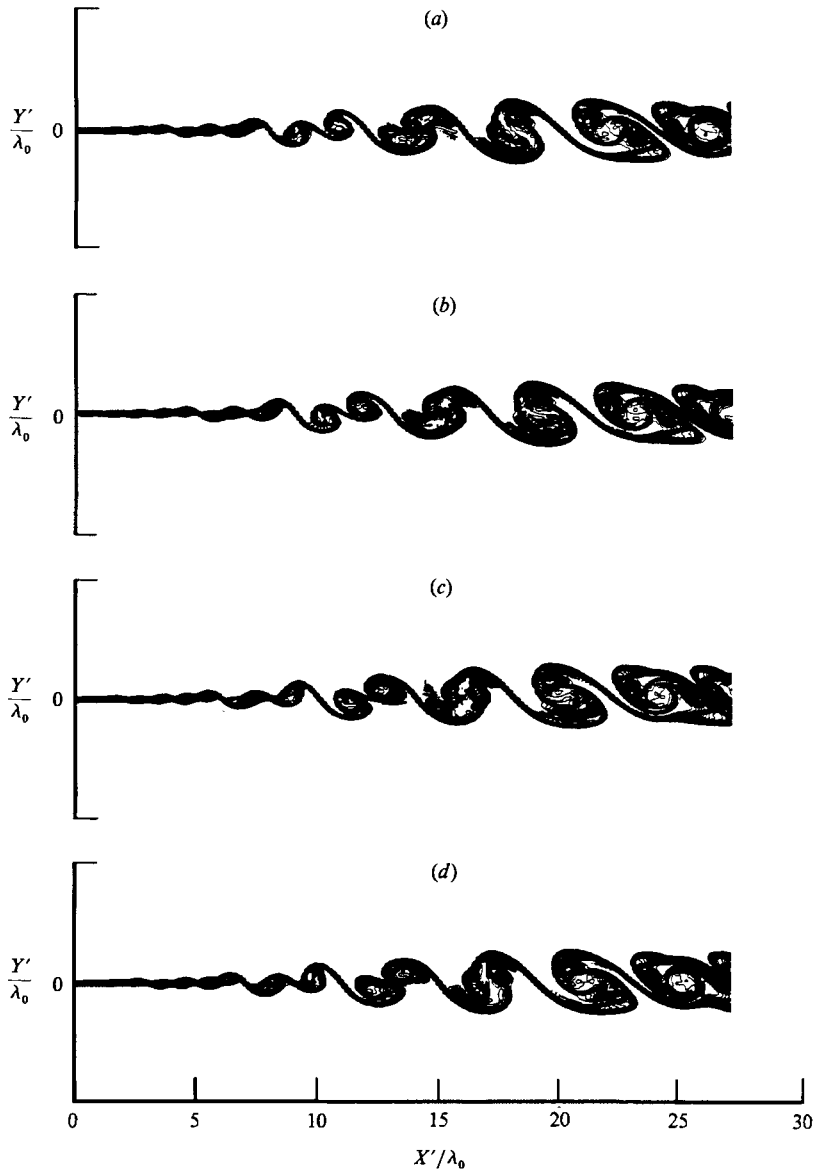

FIGURE 8. (*a–d*) Passive-scalar contours in the S-layer corresponding to four different time realizations; $\Delta U/U_m = 0.666$.

stations x', where the relative change in the amplitude and the phase difference are plotted against the crossflow direction y'. The negative values of y' correspond to the region of high-speed stream.

The feedback signal is measured downstream of the location where the fundamental has rolled-up into a vortex structure. It is in this region that the subharmonic begins to dominate since the fundamental has now saturated. Also, the feedback signal can be crucial in altering the subharmonic instability mechanism in this region. In figure 12(*a*), corresponding to $\Delta U/U_m = 2$, between the roll-up and the first pairing, i.e. $1.5 < x'/\lambda_0 < 4.0$, both amplitude and phase difference are

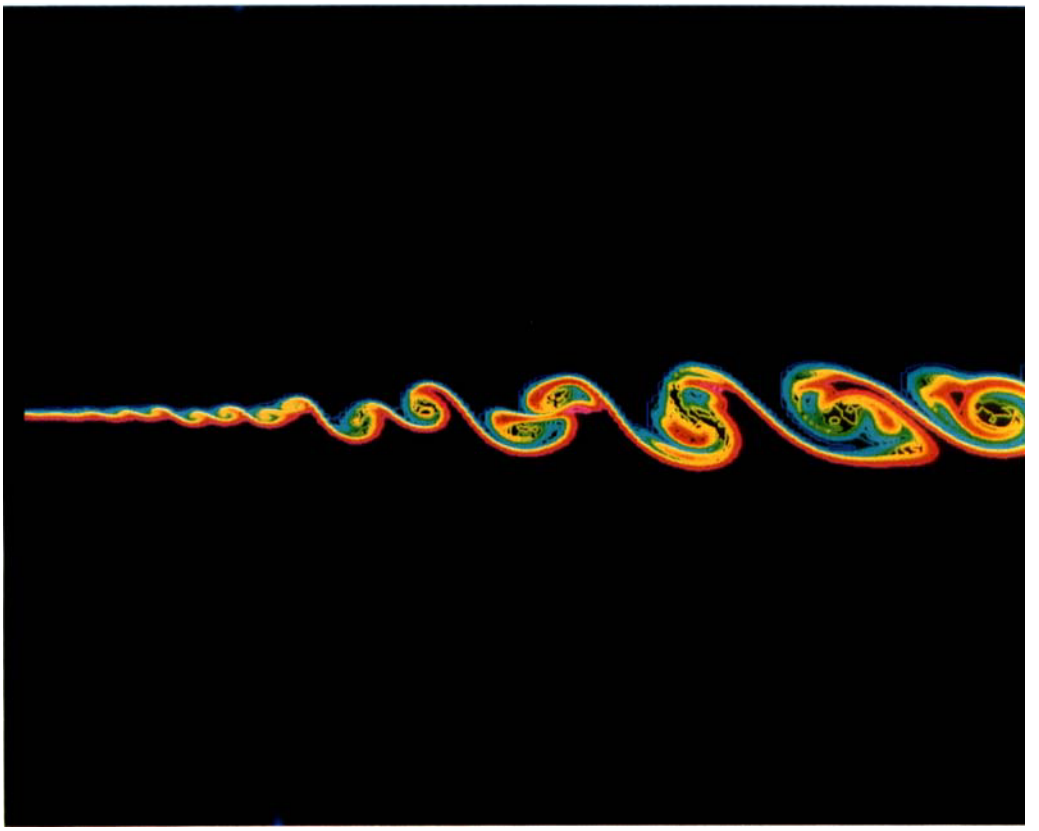

FIGURE 10. Passive-scalar contours in a mixing layer, $\Delta U/U_m = 0.666$.

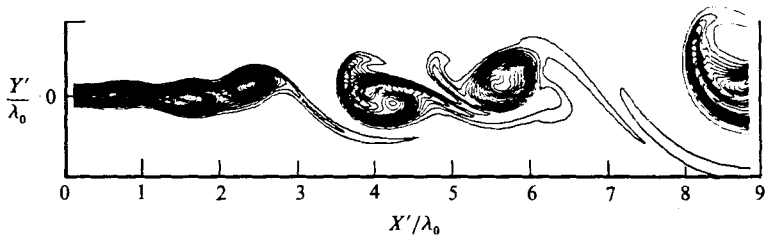

FIGURE 9. Vorticity contours in the S-layer at a given time t'; $\Delta U/U_m = 2$.

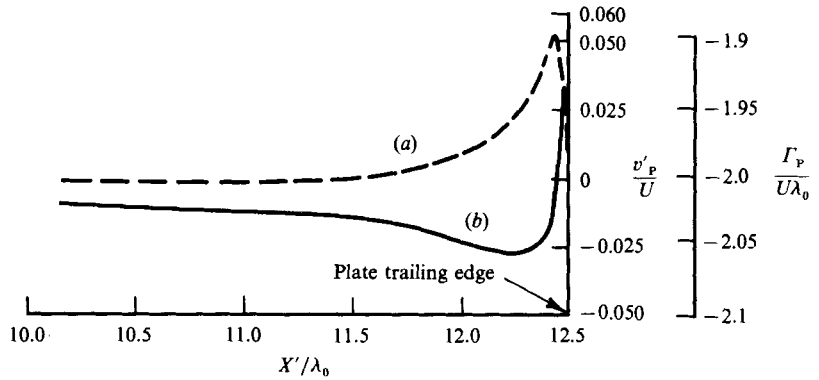

FIGURE 11. (*a*) ----, Normal velocity induced on the plate due to the mapped vorticity in the S-layer at a given time t', v'_P/U. (*b*) ——, Strength of the distributed vorticity on the plate at a given time t', $\Gamma_P/U\lambda_0$.

altered by about 10 to 15% at the midplane, $y' = 0$, between the high- and low-speed streams. Away from it, the feedback either increases or decreases, and the maximum alteration is about 30%. However, since the perturbations feed on the shear, their effect will be predominant near the midplane because of the presence of the maximum mean velocity gradient there. It is, therefore, expected that the subharmonic instability is not altered appreciably even though the feedback away from the midplane is not small. In figure 12(*b*), corresponding to $\Delta U/U_m = 0.666$, feedback is negligible everywhere; the maximum value between the roll-up ($x'/\lambda_0 = 4.5$) and the first pairing ($x'/\lambda_0 = 12.0$) is about 10%.

In their mixing-layer experiment at $\Delta U/U_m \approx 1.3$, Dimotakis & Brown (1976) detected the feedback through the velocity-fluctuation spectra which showed the presence of a frequency of the order of L/U_m for all $x' \in [0, L]$. This corroborated their hypothesis that even though the induced field at a point due to a given vortical structure downstream decays as $1/x$, as it moves further downstream the circulation around it increases linearly downstream on the average and therefore its influence at that point will not decay. However, whereas the total induced field at a given point may be strong, its contribution to the subharmonic of interest here may not be. It is this particular contribution of the induced field that is of interest in this study.

In modelling the initial development of axisymmetric turbulent jet flows at low Mach numbers, Laufer & Monkewitz (1980) used the following argument based on a feedback mechanism. The time taken by an incipient vortex to reach the location where it pairs and the time taken by the ensuing acoustic disturbance to travel upstream to the origin is equal to the time period of the subharmonic corresponding to this pairing event. They thus calculated the locations of first, second and third

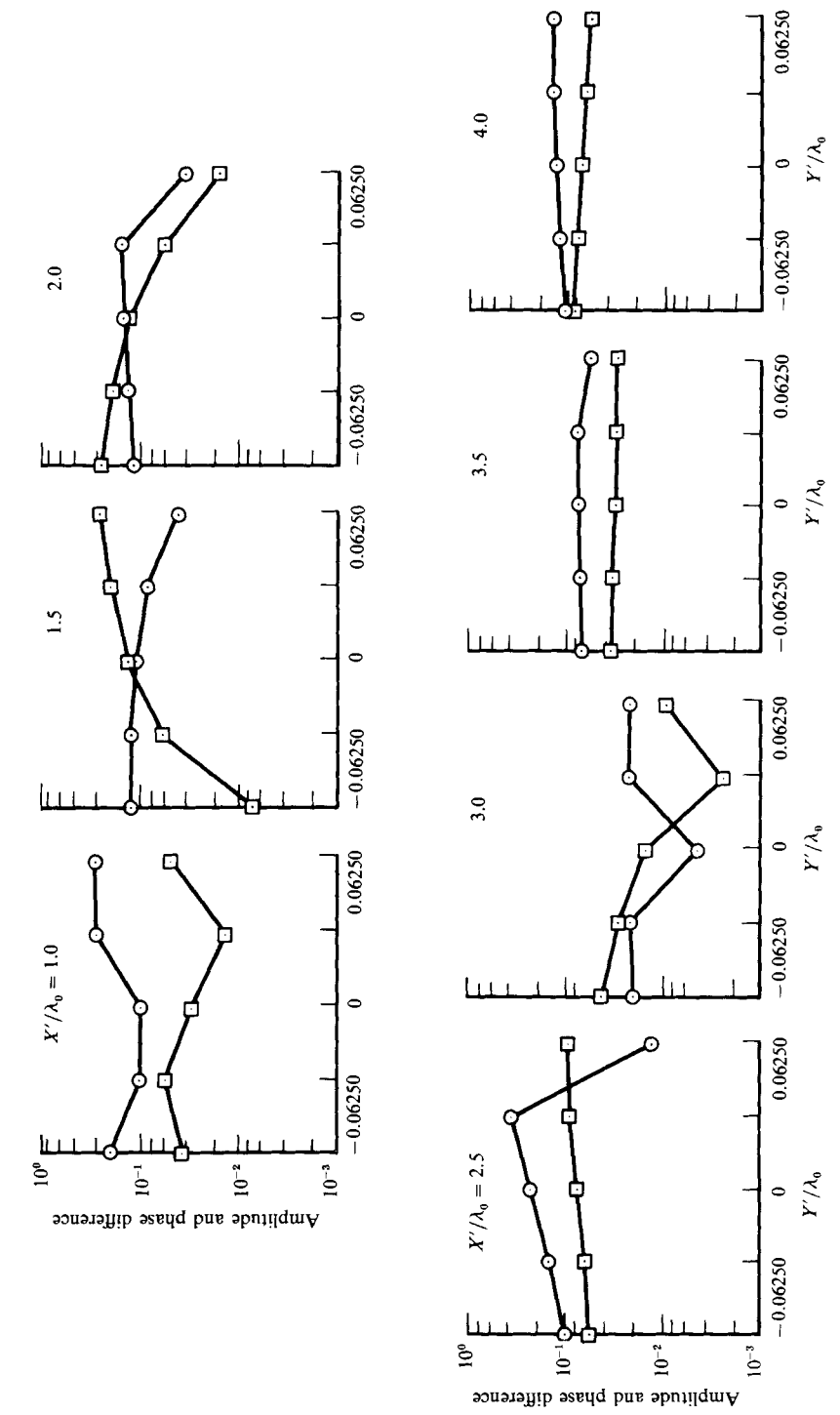

FIGURE 12 (*a*). For caption see facing page.

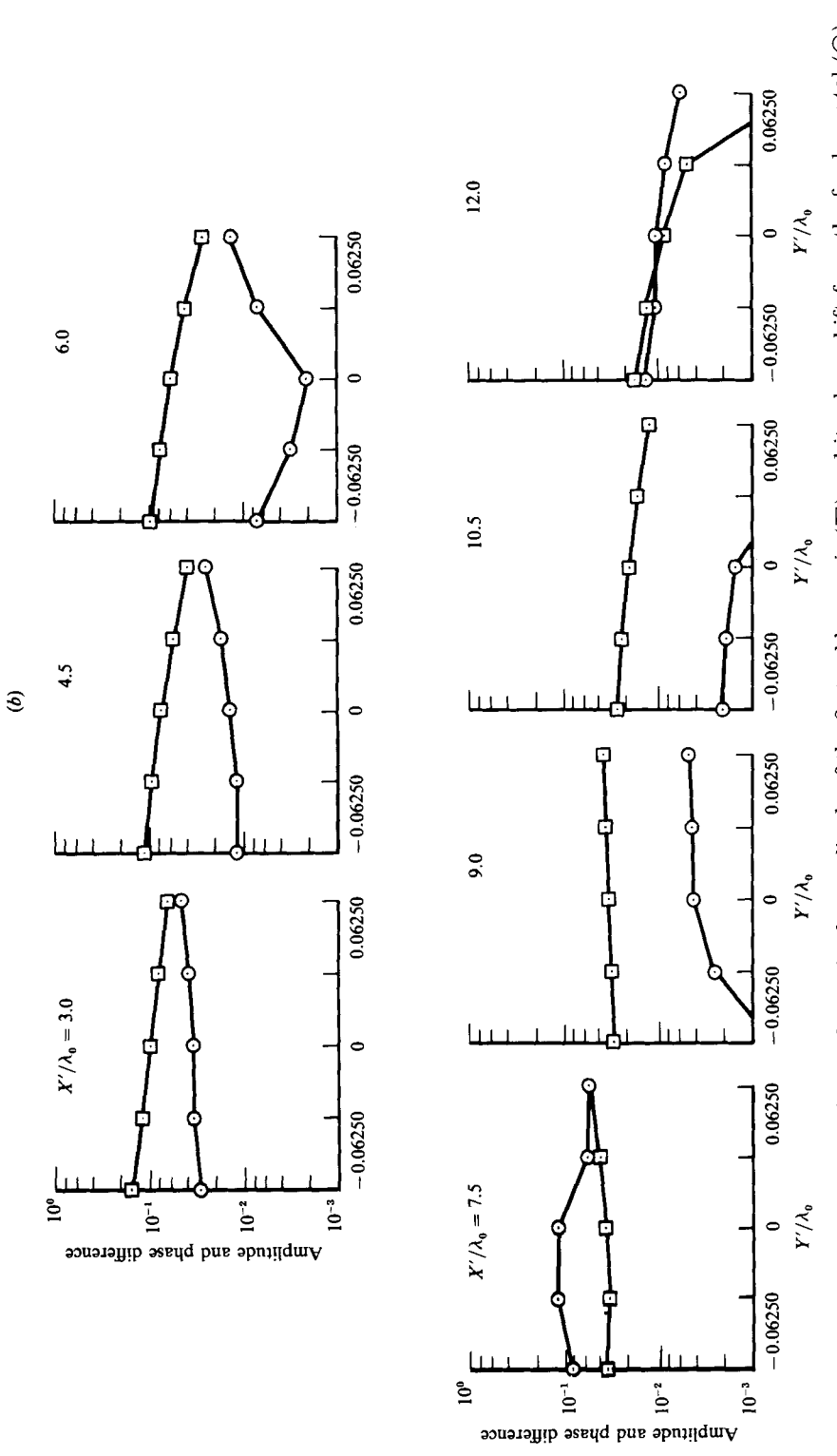

FIGURE 12. Feedback in the S-layer: relative change in the amplitude of the first subharmonic (⊡) and its phase shift from the fundamental (⊙): (*a*) $\Delta U/U_m = 2.0$, (*b*) 0.666.

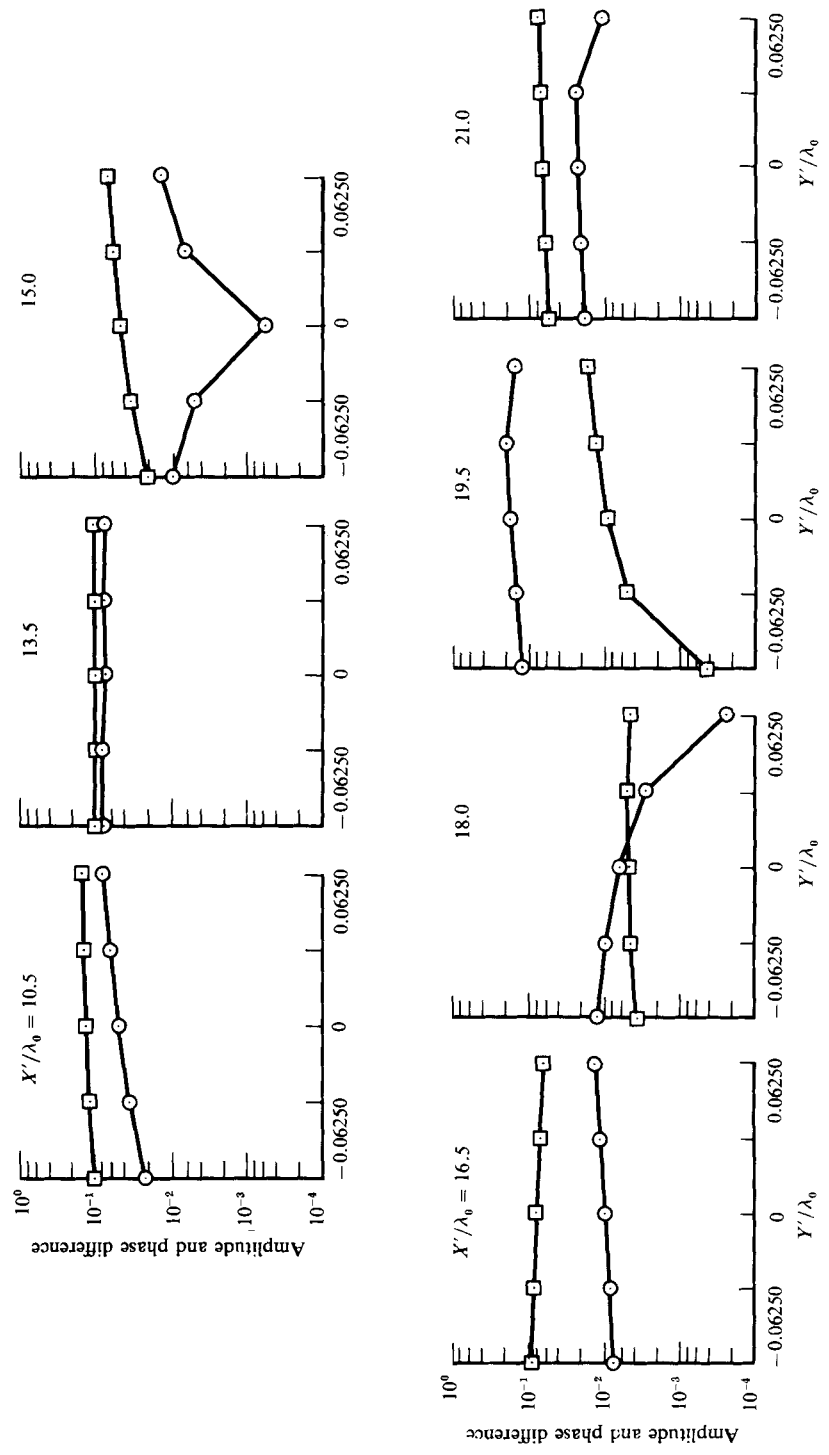

FIGURE 13. Feedback in the S-layer: Relative change in the amplitude of the third subharmonic (⊡) and its phase shift from the first subharmonic (⊙).

subharmonics, in close agreement with those given by the experiment of Kibens (1980). This suggests that the feedback is significant in the case of axisymmetric jets ($\Delta U/U_m = 2.0$).

The results presented in this study should be in error for large values of $\Delta U/U_m$, since the error of the transformations is $O(\Delta U/6U_m)$, as discussed earlier. However, according to the present model, the feedback for the largest possible value of $\Delta U/U_m = 2.0$ is larger, in general, than that for $\Delta U/U_m = 0.666$. This result is in agreement, in spirit, with the predictions of Laufer & Monkewitz (1980) and the findings of Dimotakis & Brown (1976), for large values of $\Delta U/U_m$.

Results corresponding to the feedback effect on the interaction between the first and the third subharmonics are shown in figure 13. The variation in the amplitude of the third subharmonic and the phase difference between it and the first subharmonic are plotted versus y' for various streamwise stations between the locations where the first and the second pairings are complete. Of course, as we approach the location of the second pairing, the feedback prediction becomes crude since the signal from downstream does not contain any lower imposed subharmonics, and therefore does not properly reflect the elliptic influence from downstream. However, closer to the location of the first pairing, the results as shown in figure 13 are accurate and the feedback is about 10 to 15%.

The present study has been carried out at a Reynolds number of 50 based on the initial shear-layer thickness, or 730 based on the fundamental wavelength. This represents a moderately large Reynolds number. It has been shown by Davis & Moore (1985) that as the Reynolds number is increased, the presence of feedback becomes appreciable so that the vortices do roll-up even if the forcing near the origin is stopped after a brief initial interval. Although this argument does not automatically extend to the feedback with regard to the subharmonic instability, it can be expected that for a given value of $\Delta U/U_m$, as the Reynolds number increases, the feedback of interest here may also increase, since the physical diffusion becomes smaller.

To check the dependence of feedback on the forcing levels, feedback predictions are made at two different sets of forcing levels with the fundamental amplitude fixed; in the first one, both the first and third subharmonics are at the same amplitude as the fundamental; in the second one, the first subharmonic is set at half the amplitude of the fundamental and the second at half that of the first subharmonic. The predictions in the two cases do not indicate any dependence on the forcing levels for small $\Delta U/U_m$. However, the forcing levels are well within the limit where linear theory would hold and are such as would give the fundamental a chance to amplify on its own before its first subharmonic begins to overtake it. In situations where the subharmonic is imposed at a higher forcing level than the fundamental, especially for large $\Delta U/U_m$, it can be expected that the feedback would show a dependence on the forcing levels. In the case of 'naturally' perturbed layers, the spectrum of perturbation frequencies is also biased depending on the physical environment near the origin. If the forced mixing layer develops downstream in a similar fashion as that perturbed naturally, see figure 10, it can be expected that the forcing near the origin is similar in the two cases, except for any local background noise that will supplement the instability in the latter case as it proceeds downstream in the absence of any appreciable feedback. This is suggested by the computational study of subharmonic instability of mixing layers by the author (Kaul 1986*b*).

4. Conclusions

This study deals mainly with the strength of the subharmonic disturbances that the large vortices further downstream in a mixing layer can induce on the flow upstream. This feedback effect has been found to be relatively small, at least for small velocity ratios. The induced effect of the vorticity distribution is also a measure of the ellipticity of the governing equations for the mixing layer. Thus we expect that the streamwise developing layer is only weakly elliptic, at least for small velocity ratios. The results suggest that the perturbations that control the growth of the subharmonics and therefore of the shear layer itself are not primarily caused by the developing instability of the layer itself but by external disturbances. It follows that the rate of growth of a natural layer should depend on more than the value of $\Delta U/U_{\mathrm{m}}$. The spectral content of the random perturbations of the flow near the origin of the layer should influence its growth, and only for two layers for which this spectral content is dynamically similar should one expect similarity downstream. Perhaps the lack of agreement between experimentalists about the growth rate, e.g. Liepman & Laufer (1947), Brown & Roshko (1974), Miles & Shih (1968), Patel (1973), Mills (1968), Spencer & Jones (1971), Wygnanski & Fiedler (1970), and the evidence of the large effect of the initial conditions on the growth rate (Weisbrot, Einav & Wygnanski 1982; Ho & Huang 1982) are related to this sensitivity of the layer dynamics to initial conditions. Thus the traditional view of the mixing layer as a self-similar flow may need re-examination.

A unique method to calculate the spatially growing mixing-layer vorticity field has been developed which clearly captures the distribution of vorticity realistically for small values of velocity ratios. The method does not suffer from the ill-posedness of the direct simulation methods for the spatially growing mixing layers in that no arbitrary inflow and outflow conditions have to be imposed, and that there is no contamination of initially imposed linear perturbations by the truncation-error terms of a finite-difference scheme. The inflow conditions for the present method derive themselves out of the transformation and include the contribution from the feedback signal. The method offers us the unique ability to measure the feedback signal in the spatially growing mixing layer and thus in having *a priori* knowledge of the appropriate perturbation required to be imposed at the origin of the flow for a given mixing-layer growth rate. This does not seem to be possible otherwise. Also, the method can provide the inflow and outflow conditions for a direct simulation of the spatially growing mixing layer, which, in principle, are not available otherwise, e.g. the outflow boundary condition must be of the properly reflecting type rather than of the non-reflecting type.

Various extrapolation outflow boundary conditions in the S-layer can be derived using the transformations proposed here. For example, a parabolic extrapolation boundary condition in the T-layer, $u_t = 0$, would transform to an appropriate downstream boundary condition, $u'_{t'} + U_{\mathrm{m}} u'_{x'} = 0$ in the S-layer.

Although the total vorticity-induced field in the mixing layer is not necessarily small, its effect on the subharmonic instability is seen to be small in the neighbourhood of the midplane between the high- and low-speed sides of the mixing layer, even for the largest possible value of $\Delta U/U_{\mathrm{m}}$ (one stream at rest). Since the transformation becomes progressively less accurate as the velocity ratio increases, the feedback prediction for $\Delta U/U_{\mathrm{m}} = 2$ is not very accurate. However, for small $\Delta U/U_{\mathrm{m}}$, it has been quantitatively shown that the feedback in a forced mixing layer is small. As a result, the proposed transformations offer the novel capability of

studying the spatially growing mixing layers (Kaul 1986*b*) with small velocity ratios.

The author is grateful to Professor Gilles M. Corcos for helpful discussions during the course of this study, and to Professor Maurice Holt for the insight he gained from his courses on Numerical Methods in Fluid Dynamics at Berkeley and his continuous interest in this research work. This work was partially supported by the National Science Foundation, the University of California Chancellor's Patent Fund Award and the NASA Ames Research Center under contract NAS2-11555.

REFERENCES

ASHURST, W. T. 1977 Numerical simulation of turbulent mixing layers via vortex dynamics. In *Turbulent Shear Flows* (ed. F. Durst, B. E. Launder, F. W. Schmidt & J. H. Whitelaw), p. 402. Springer.

BATT, R. G. 1975 Some measurements on the effect of tripping the two-dimensional shear layer. *AIAA J.* **2**, 245.

BROWAND, F. K. 1966 An experimental investigation of an incompressible, separated shear layer. *J. Fluid Mech.* **26**, 281.

BROWN, G. R. & ROSHKO, A. 1974 On the density effects and large structure in turbulent mixing layers. *J. Fluid Mech.* **64**, 775.

BRADSHAW, P. 1966 The effect of initial conditions on the development of a free shear layer. *J. Fluid Mech.* **26**, 225.

CHORIN, A. J. 1973 Numerical study of slightly viscous flow. *J. Fluid Mech.* **57**, 785.

COLES, D. 1985 On the uses of coherent structures. *AIAA Dryden Lecture, 23rd AIAA Aerospace Sciences Meeting, January, Reno, Nevada.*

CORCOS, G. M. 1979 The mixing layer: deterministic models of a turbulent flow, Rep. FM-79-2. University of California, Berkeley.

CORCOS, G. M. 1980 The deterministic description of the coherent structure of free shear layers. *Intl Conf. on Coherent Structure in Turbulent Shear Flow, Madrid, Spain.* Lecture Notes in Physics, vol. 136, p. 10, Springer.

CORCOS, G. M. & SHERMAN, F. S. 1976 Vorticity concentration and the dynamics of unstable free shear layers. *J. Fluid Mech.* **73**, 241.

CORCOS, G. M. & SHERMAN, F. S. 1984 The mixing layer: deterministic models of a turbulent flow. Part 1. Introduction and the two-dimensional flow. *J. Fluid Mech.* **139**, 29.

DAVIS, R. W. & MOORE, E. F. 1985 A numerical study of vortex merging in mixing layers. *Phys. Fluids* **28**, 1626.

DIMOTAKIS, P. E. & BROWN, G. L. 1976 The mixing layer at high Reynolds number: large-structure dynamics and entrainment. *J. Fluid Mech.* **78**, 535.

FAVRE, A., GAVIGLIO, J. & DUMAS, R. 1967 Structure of velocity space–time correlations in a boundary layer. *Phys. Fluids* **10**, S138.

FREYMUTH, P. 1966 On transition in a separated laminar boundary layer. *J. Fluid Mech.* **25**, 683.

FUJIWARA, T., TAKI, S. & ARASHI, K. 1986 Numerical analysis of a reacting flow in H2/O2 rocket combustor. Part 1: Analysis of turbulent shear flow. *AIAA Paper* 86-0528, *AIAA 24th Aerospace Sciences Meeting, January 1986.*

GASTER, M. 1962 A note on the relation between temporally-increasing and spatially-increasing disturbances in hydrodynamic stability. *J. Fluid Mech.* **14**, 222.

GASTER, M. 1965 The role of spatially growing waves in the theory of hydrodynamic stability. *Prog. Aero. Sci.* **6**, 251.

HO, C.-M. & HUANG, L.-S. 1982 Subharmonics and vortex merging in mixing layers. *J. Fluid Mech.* **119**, 443.

JIMÉNEZ, J. 1980 On the visual growth of a turbulent mixing layer. *J. Fluid Mech.* **96**, 447.

KAUL, U. K. 1982 Do large vortices control their own growth in a mixing layer? An assessment by a boot-strap method. Ph.D. thesis, University of California, Berkeley, Mech. Engng Dept.

KAUL, U. K. 1986*a* A numerical method to assess the feedback in a free shear layer. In *Proc. Tenth Intl Conf. on Numerical Methods in Fluid Dynamics, Beijing, China, June 23–27*. Lecture Notes in Physics, vol. 264, p. 369, Springer.

KAUL, U. K. 1986*b* A computational study of the subharmonic instability in mixing layers. *Proc. Tenth US National Congress of Applied Mechanics, The University of Texas at Austin, Austin, Texas, June 16–20* (ed. J P. Lamb), p. 545. ASME.

KIBENS, V. 1980 Discrete noise spectrum generated by an acoustically excited jet. *AIAA J.* **18**, 434.

LAUFER, J. & MONKEWITZ, P. 1980 On turbulent jet flows: a new perspective. *AIAA Paper* 80-0962.

LIEPMAN, H. W. & LAUFER, J. 1947 Investigation of free turbulent mixing. *NACA Tech. Note* 1257.

MILES, J. B. & SHIH, J. 1968 Similarity parameter for two-stream turbulent jet-mixing region. *AIAA J.* **6**, 1429.

MILLS, R. D. 1968 Numerical and experimental investigations of the shear layer between two parallel streams. *J. Fluid Mech.* **33**, 591.

MONKEWITZ, P. A. & HUERRE, P. 1982 The influence of the velocity ratio on the spatial instability of mixing layers. *Phys. Fluids* **25**, 1137.

PATEL, R. P. 1973 An experimental study of a plane mixing layer. *AIAA J.* **11**, 67.

PATNAIK, P. C., CORCOS, G. M. & SHERMAN, F. S. 1976 A numerical simulation of Kelvin–Helmholtz waves of finite amplitude. *J. Fluid Mech.* **73**, 215.

PELTIER, W. R., HALLE, J. & CLARKE, T. L. 1978 The evolution of finite amplitude Kelvin–Helmholtz billows. *Geophys. Astrophys. Fluid Dyn.* **10**, 53.

PUI, N. K. & GARTSHORE, I. 1978 Measurements of the growth rate and structure in plane turbulent mixing layers. *J. Fluid Mech.* **91**, 111.

RILEY, J. J. & METCALFE, R. W. 1980 Direct numerical simulation of a perturbed turbulent mixing layer. *AIAA Paper* 80-0274, *AIAA 18th Aerospace Sciences Meeting, Jan. 14–16, Pasadena, California.*

SPENCER, B. W. & JONES, B. G. 1971 Statistical investigation of pressure and velocity fields in the turbulent two-stream mixing layer. *AIAA Paper* 71, p. 613.

THORPE, S. A. 1971 Experiments on the instability of stratified shear flows: miscible fluids. *J. Fluid Mech.* **46**, 299.

WEISBROT, I., EINAV, S. & WYGNANSKI, I. 1982 The nonunique rate of spread of the two-dimensional mixing layer. *Phys. Fluids* **25**, 1691.

WINANT, C. D. & BROWAND, F. K. 1974 Vortex pairing: the mechanics of turbulent mixing layer growth at moderate Reynolds numbers. *J. Fluid Mech.* **63**, 237.

WYGNANSKI, I. & FIEDLER, H. E. 1970 The two-dimensional mixing region. *J. Fluid Mech.* **41**, 327.